

# Etch pit morphology and magnesium inhibition of calcite dissolution

R. S. Arvidson, K. J. Davis, M. Collier & A. Lutge

*Department of Earth Science MS-126, Rice University, Houston, TX, 77005 USA*

J. E. Amonette

*Environmental Molecular Sciences Laboratory, Pacific Northwest National Laboratory, MS K8-93, P.O. Box 999, Richland, WA 9935 USA*

**ABSTRACT:** Mg inhibition of calcite dissolution is observed in simple carbonated solutions in single crystal experiments. Although inhibition of the overall rate occurs at relatively low Mg concentrations, increasing concentrations give rise to progressive changes in the morphology of etch pits. These observations can be understood in the context of changes in the relative rates of double kink nucleation and single kink propagation rates on step edges, tentatively attributed to site-specific surface adsorption of  $\text{MgHCO}_3^+$  or  $\text{MgCO}_3^\circ$ .

## 1 INTRODUCTION

### 1.1 *Recent progress in carbonate mineral dissolution kinetics*

Significant progress has been made in understanding the mechanistic details of dissolution dynamics on the (104) cleavage surface of carbonate minerals. Much of this recent work has focused on AFM observations of the rate of step and kink movement (e.g. Liang et al. 1996a, b, Jordan & Rammensee 1998, Lea et al. 2001, Higgins et al. 2002). Observations of dissolution rates over larger lateral scales have also provided basic insight into the relationships of etch pit development and defect distribution (MacInnis & Brantley 1992, 1993, Lutge et al. 2003), as well as comparison with the overall “bulk” rate measured in mineral powders (Arvidson et al. 2003). In addition, considerable insight has been generated by integrating surface complexation models and observations (Van Cappellen et al. 1993, Stipp et al. 1994, Pokrovsky et al. 1999, Fenter et al. 2000, Pokrovsky & Schott 2002) with an atomistic description of surface topography and measurement of step velocities (Duckworth & Martin 2003). This general approach also has the potential to yield substantial detail regarding inhibition mechanisms in dissolution reactions as well. In this brief paper, we describe preliminary experimental observations of magnesium inhibition of calcite dissolution, and suggest how this inhibition may be related mechanistically to site-specific surface properties.

### 1.2 *Previous work on Mg inhibition of calcite dissolution*

Previous data on magnesium inhibition of calcite dissolution kinetics have been derived almost entirely through conventional experiments using mineral powders. These early data in general confirm inhibition, but differ in terms of the concentration required to impose a given reduction in rate. These variations most likely reflect the inherent diversity of experimental conditions: pH,  $\Delta G_r$ , ionic strength, composition of supporting electrolytes, solid phase characteristics, and other factors (e.g. Berner 1967). Subsequent to work on trace metal inhibition by Terjesen et al. (1961) and Nestaas & Terjesen (1969), Sabbides & Koutsoukos (1995) observed dissolution to be inhibited at  $\text{Mg}^{2+}$  concentrations between 40 and 460  $\mu\text{M}$  (rates reduced by 0.3 and 0.5  $\log_{10}$  units, respectively) in experiments performed close to calcite saturation. In contrast, although Gutjahr et al. (1996) found a reduction in calcite *growth* rates, they found Mg to have no effect on dissolution at concentrations of 300  $\mu\text{M}$   $\text{Mg}(\text{NO}_3)_2$ . In dilute, mixed  $\text{Mg}^{2+}$ - $\text{Ca}^{2+}$  solutions, Sjöberg (1978) concluded inhibition of calcite dissolution to be sufficiently complex as to preclude incorporation of both these components in a general rate equation. Compton & Brown (1994) found a significant reduction in rate in the presence of 10 – 80 mM  $\text{Mg}^{2+}$ , (~50% at 40 mM, pH 8 – 9), which they found to be consistent with a Langmuir-Volmer adsorption isotherm. Alkattan et al. (2002) studied dissolution of calcite *single crystals* in rotating disk experiments and found no inhibition at  $\text{MgCl}_2$  concentrations up to 0.1 molal (pH 1 – 3).

## 2 METHODS

We measured Mg inhibition of calcite dissolution on single crystal (104) surfaces by two approaches. Absolute surface-normal retreat rates were derived from time-lapse changes in surface topography by *ex situ* vertical scanning interferometry (VSI), after flowing reactant solution over this surface in a fluid microcell (for details, see Lutge et al. 1999, 2003, Arvidson et al. 2003). This method allowed quantitative mapping of relatively large areas of the mineral surface at subnanometer vertical resolution (Fig. 1). The second approach involved monitoring similarly prepared calcite surfaces with reactant solutions in an AFM flow cell (Digital Instruments Nanoscope III Multimode SPM, operated in contact mode). All experiments used cleavage rhombs derived from high purity synthetic calcite. Carbonated reactant solutions were prepared from  $\text{Na}_2\text{CO}_3$  or  $\text{NaHCO}_3$  (4.4 meq/L) continuously equilibrated with atmospheric  $\text{CO}_2$  (pH 8.8 – 9.0, 25°C; cf. Liang et al. 1996b, Lea et al. 2001). Mg was added (as  $\text{MgCl}_2$ ) in concentrations of 0, 10, 50, 300, and 800  $\mu\text{M}$ . Additional experiments were also performed as a function of pH in  $\text{N}_2$ -sparged ( $\text{CO}_2$ -free) solutions at the same ionic strength and  $\text{MgCl}_2$  concentrations.

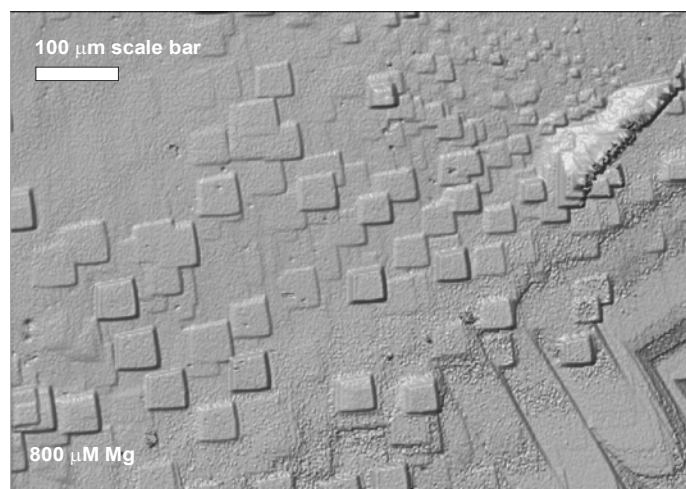


Figure 1. VSI data (10 $\times$  magnification, white light) from coalescing etch pits on calcite (104) surface, reacted in 4.4 mM  $\text{NaHCO}_3$ , 800  $\mu\text{M}$   $\text{MgCl}_2$ , maintained at pH  $\sim$  9,  $\text{PCO}_2 \sim 10^{-3.5}$ , 25°C. Positive step directions  $[-441]_+$  and  $[48-1]_+$  are oriented to the right and down, respectively.

## 3 RESULTS AND DISCUSSION

In our VSI runs, we observed that inhibition occurs in carbonated solutions (pH  $\sim$ 9) at relatively low concentrations: relative to the rate in Mg-free  $\text{NaHCO}_3$  solution, the addition of 10  $\mu\text{M}$   $\text{MgCl}_2$  reduces the dissolution rate by  $\sim$ 80%, and 300  $\mu\text{M}$  reduces the rate by  $\sim$ 90%. At higher concentrations, under conditions in which the solution is supersaturated with respect to pure magnesite, we observed that etch pit morphology departed significantly from

the symmetrical rhombic shape observed in Mg- and  $\text{CO}_2$ -free solutions. Etch pit morphologies in carbonated Mg-free solutions (pH  $\sim$  9) showed rounding at the intersection of the obtuse (+) step edges, such that the radius of the (+) steps decrease toward their common terminus. Lea et al. (2001) showed this morphology to be associated with a reduction in (+) step velocity, and attributed this inhibition to probable adsorption of carbonate ion at (+,+) kink sites. In our experiments, carbonated solutions having the highest ( $\sim$ 800  $\mu\text{M}$ ) Mg concentrations produced (+,+) step intersections that remained relatively sharp but instead curved toward the (+,-) step intersections (Fig. 1). These changes implied changes in kink density along step edges, and variations in the kink nucleation rate.

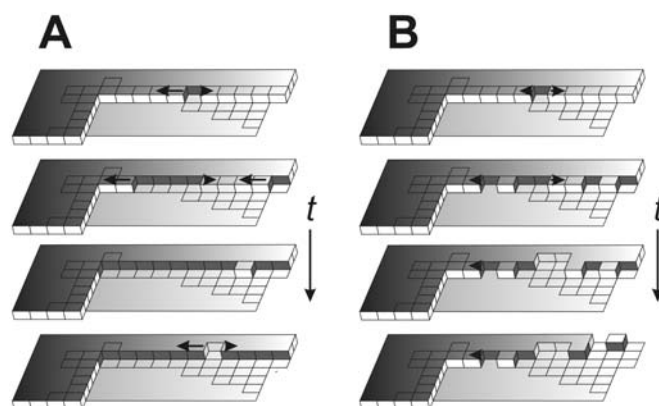


Figure 2. Evolution of step edges showing relationships between double kink nucleation rate ( $R_{KK}$ ), kink migration rate ( $R_K$ ), kink density, and step movement (adapted from Liang et al. 1996a). Time  $t$  increases from top to bottom. (A) In order for steps to remain straight, kink density must remain low: either no new double kinks can nucleate prior to the exit of single kinks at the step terminus (self annihilation), or single kinks formed from adjacent double kinks must annihilate each other (kink-kink annihilation). In both cases,  $R_K$  must remain high relative to  $R_{KK}$ . (B) Rough, irregular step profiles should thus result from inhibition of  $R_K$  relative to  $R_{KK}$ . “Curved” step profiles can be produced by a coupled reduction in  $R_K$  relative to  $R_{KK}$  and a pronounced anisotropy in single kink migration rates, i.e.  $R_{K+} \neq R_{K-}$ .

Step curvature and roughness can be understood in the context of the rate of two related processes: double kink nucleation ( $R_{KK}$ ) and single kink propagation of either positive ( $R_{K+}$ ) or negative ( $R_{K-}$ ) kink sites. As shown in Figure 2, if  $R_{KK}$  is slow relative to  $R_K$ , then kinks will tend to annihilate one another before new kinks can form. Conversely, if  $R_K$  is reduced to the point where  $R_{KK}$  is competitive, then existing kinks may be preserved prior to the next cycle of kink nucleation. Liang et al. (1996a) elegantly demonstrated that simple kink annihilation at the step terminus was insufficient to explain both straight step morphology and constant step velocity, and postulated that the persistence of straight steps must reflect a balance between  $R_{KK}$  and the annihilation of adjacent kink pairs.

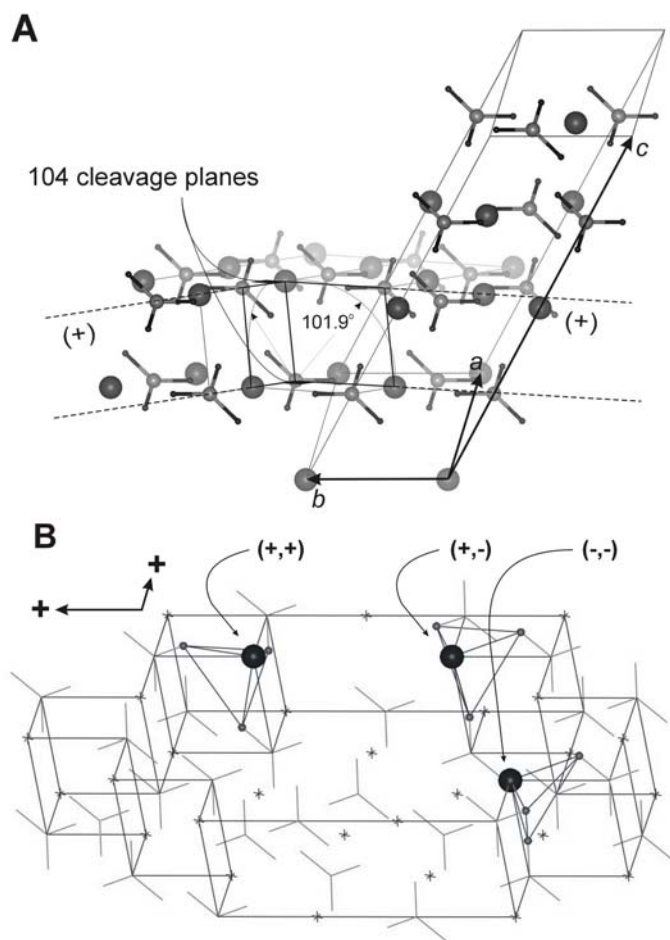


Figure 3. Calcite 104 cleavage surface. (A) Orientation of cleavage planes, hexagonal unit cell, obtuse (+) step faces, Ca atoms (large gray), and trigonal  $\text{CO}_3$  groups. Out-of-plane, in-plane, and below-plane oxygens coordinate each carbon atom. (B) Ca-O coordination at kink sites, showing monatomic etch pit (black outline), trigonal  $\text{CO}_3$  groups (gray), and Ca atoms (shown either as large black atoms, stars, or omitted for clarity). The length of Ca-O bonds between surface calciums (large black) and coordinating oxygens (small gray) at different kink sites have the same length. However, oxygen-oxygen distances within these truncated coordination octahedra are not equivalent: oxygens coordinating Ca at the (+,+) surface site all have O-O distances of 3.26Å, whereas O-O distances associated with (+,-) and (-,-) sites are mixed (3.26 and 3.41Å).

Morphologic changes occur at Mg concentrations substantially greater than those required to induce significant overall inhibition. Because movement of the “fast” (+) steps is responsible for much of the bulk dissolution (Liang et al. 1996b), inhibition at these sites may occur with relatively little inhibitor addition, similar to the effect observed for dissolved carbon and  $\text{Mn}^{2+}$  (Lea et al. 2001, Arvidson et al. 2003). It is unlikely that these morphologies reflect simple adsorption of dehydrated  $\text{Mg}^{2+}$  ions at specific kink sites, as they were not observed in  $\text{CO}_2$ -free solutions (pH 8 – 11+). Formation of ion pairs  $\text{MgCO}_3^0$  or  $\text{MgHCO}_3^+$  scavenge free carbonate ion from solution, and thus may reduce the carbonate ion concentration at kink sites. These components (as well as  $\text{Mg}^{2+}$ ) may also form significant surface complexes as well, and their interactions result in overall inhibition (Arvidson et al., in prep.).

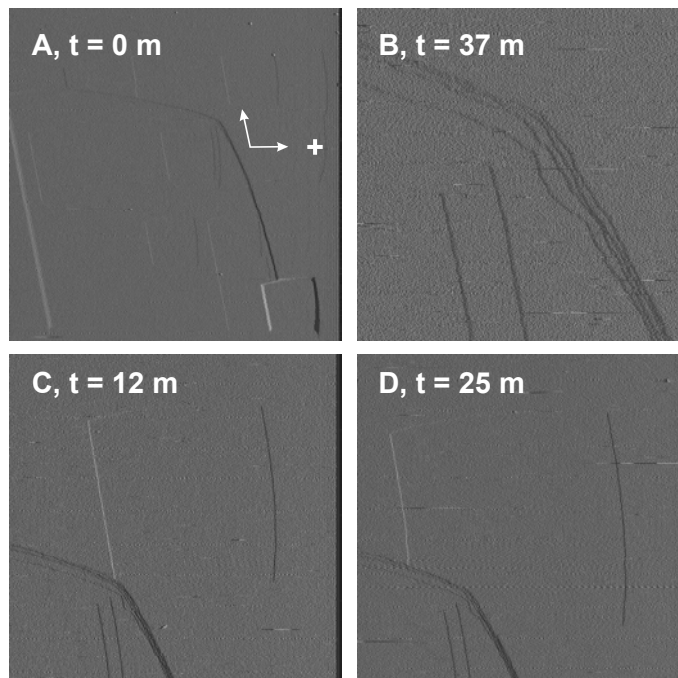


Figure 4. AFM reaction sequence. (A)  $10 \times 10 \mu\text{m}$  image of large etch pit previously formed in Mg-free solution, showing “ $\text{CO}_3^-$ ” inhibition of obtuse (+) step directions by rounding towards the (+,+) intersection. Etch pit at lower right formed immediately after introduction of  $800 \mu\text{M}$   $\text{MgCl}_2$ . (B)  $1 \times 1 \mu\text{m}$  image detail of (+,+) corner (left of arrows in A), contrasting rough step edges of “ $\text{CO}_3^-$ ”-inhibited etch pit with those of newly formed pit (appearing after  $\text{MgCl}_2$  introduction) having sharp (+,+) corners. (C, D) Growth of etch pit via advance of acute (-) steps in  $800 \mu\text{M}$   $\text{MgCl}_2$  solution, showing coalescence with static (+,+) intersection of older etch pit. Scan field is  $3 \times 3 \mu\text{m}$ .

The basic anisotropy of obtuse versus acute step velocities on the calcite surface may reflect a complex interaction between the energetics of removal of cationic and anionic components broadly mediated by dominant surface complex populations ( $>\text{MOH}_2^+$  versus  $>\text{CO}_3\text{H}$ ; Duckworth & Martin, 2003). Because of the oblique orientation of carbonate groups with respect to the (104) surface, these sites differ in terms of coordination. For example, although removal of surface calcium demands cleavage of Ca-O bonds, the O-O distances within the surface-truncated Ca-octahedra vary according to their crystallographic orientation at (+,+), (+,-) and (-,-) metal sites (Fig. 3).

The relationship of step movements and inhibition can also be clarified by study of time-lapse AFM data. Figure 4 shows a sequence in which a previously developed etch pit, grown in carbonated Mg-free solution, is the site of new etch pit formation upon introduction of  $800 \mu\text{M}$  carbonated  $\text{MgCl}_2$  into the flow cell. This sequence definitively shows that (1) the (+) steps are severely inhibited after Mg introduction, with little measurable advance, and (2) growth of new etch pits occurs by advance of (-) steps. Although dissolved carbon (“ $\text{CO}_3^-$ ”, Fig. 4) reduces (+) step velocities (Lea et al. 2001), the fact that step curvature towards the (+,+) corner, previ-

ously developed under Mg-free conditions, is retained, while newly formed pits at 800  $\mu\text{M}$   $\text{MgCl}_2$  show relatively sharp (+,+) corners, suggests that the (+) steps are fully passivated, and that the rates of both double kink nucleation and single kink migration along either  $[48-1]_+$  or  $[-441]_+$  are low. Curvature of the (+) steps may instead reflect ineffective kink removal at the (-,+) corner, implying that the rate of single kink migration ( $R_{K+}$ ) along the (-) steps is inhibited in the (+) direction as well. However, for the (-) steps to remain straight (Fig. 4) also implies that  $R_K \gg R_{KK}$ .

## 4 CONCLUSIONS

We have documented magnesium inhibition of calcite dissolution in alkaline solutions far from equilibrium. As is the case for dissolved carbon addition, inhibition from increasing Mg concentration is associated with unique etch pit morphologies, reflecting possible changes in the relative rates of double kink nucleation and single kink migration. These changes are also linked to dissolved carbon concentration, and may reflect interaction of Mg ion pairs with the surface. These relationships will be explored in future modeling work.

## ACKNOWLEDGEMENTS

This work was supported by the Office of Basic Energy Science, Geosciences Research Program, US Department of Energy. PNNL is a multiprogram national laboratory operated by Battelle Memorial Institute for the US Department of Energy under Contract DE-AC06-76RL0 1830.

## REFERENCES

Alkattan, M., Oelkers, E. H., Dandurand, J.-L. & Schott, J. 2002. An experimental study of calcite dissolution rates at acidic conditions and 25 °C in the presence of  $\text{NaPO}_3$  and  $\text{MgCl}_2$ . *Chem. Geol.* 190: 291–302.

Arvidson, R.S., Ertan, I.E., Amonette, J.E. & Lutge, A. 2003. Variation in calcite dissolution rates: A fundamental problem? *Geochim. Cosmochim. Acta* 67: 1623–1634.

Berner, R.A. 1967. Comparative dissolution characteristics of carbonate minerals in the presence and absence of aqueous magnesium ion. *Am. J. Sci.* 265: 45–70.

Compton, R.G. & Brown, C.A. 1994. The inhibition of calcite dissolution/precipitation:  $\text{Mg}^{2+}$  cations. *J. Colloid. Interface Sci.* 165: 445–449.

Duckworth, O.W. & Martin, S.T. 2003. Connections between surface complexation and geometric models of mineral dissolution investigated for rhodochrosite. *Geochim. Cosmochim. Acta* 67: 1787–1801.

Fenter, P., Geissbuhler, P., DiMasi, E., Srajer, G., Sorensen, L. B. & Sturchio N.C. 2000. Surface speciation of calcite observed *in situ* by high-resolution X-ray reflectivity. *Geochim. Cosmochim. Acta* 64: 1221–1228.

Gutjahr, A., Dabringhaus, H. & Lacmann, R. 1996. Studies of the growth and dissolution kinetics of the  $\text{CaCO}_3$  polymorphs calcite and aragonite: II. The influence of divalent cation additives on the growth and dissolution rates. *J. Cryst. Growth* 158: 310–315.

Higgins, S.R. Jordan, G. & Eggleston, C.M. 2002. Dissolution kinetics of magnesite in acidic aqueous solution: A hydrothermal atomic force microscopy study assessing step kinetics and dissolution flux. *Geochim. Cosmochim. Acta* 66: 3201–3210.

Jordan, G. & Rammensee, W. 1998. Dissolution rates of calcite (10-14) obtained by scanning force microscopy: Microtopography-based dissolution kinetics on surfaces with anisotropic step velocities. *Geochim. Cosmochim. Acta* 62: 941–947.

Lea, A.S., Amonette, J.E., Baer, D.R., Liang, Y. & Colton, N. G. 2001. Microscopic effects of carbonate, manganese, and strontium ions on calcite dissolution. *Geochim. Cosmochim. Acta* 65:369–379.

Liang, Y., Baer, D.R. McCoy, J.M. & LaFemina, J.P. 1996a. Interplay between step velocity and morphology during the dissolution of  $\text{CaCO}_3$  surface. *J. Vac. Sci. Technol. A* 14: 1363–1375.

Liang, Y., Baer, D.R. McCoy, J.M., Amonette, J.E. & LaFemina, J.P. 1996b. Dissolution kinetics at the calcite-water interface. *Geochim. Cosmochim. Acta* 60: 4883–4887.

Lutge, A., Bolton, E.W. & Lasaga, A.C. 1999. An interferometric study of the dissolution kinetics of anorthite: the role of reactive surface area. *Am. J. Sci.* 299: 652–678.

Lutge, A., Winkler, U. & Lasaga, A.C. 2003. An interferometric study of the dolomite dissolution: A new conceptual model for mineral dissolution. *Geochim. Cosmochim. Acta* 67: 1099–1116.

MacInnis, I.N. & Brantley, S.L. 1992. The role of dislocations and surface morphology in calcite dissolution. *Geochim. Cosmochim. Acta* 56: 1113–1126.

MacInnis, I.N. & Brantley, S.L. 1993. Development of etch pit size distributions on dissolving minerals. *Chem. Geol.* 105: 1–49.

Nestaas, I. & Terjesen, S.G. 1969. The inhibiting effect of scandium ions upon the dissolution of calcium carbonate. *Acta Chem. Scand.* 23: 2519–2531.

Pokrovsky, O.S., Schott, J. & Thomas F. 1999. Processes at the magnesium bearing carbonates/solution interface. I. A surface speciation model for magnesite. *Geochim. Cosmochim. Acta* 63:863–880.

Pokrovsky, O.S. & Schott, J. 2002. Surface chemistry and dissolution kinetics of divalent metal carbonates. *Environ. Sci. Technol.* 36:426–432.

Sabbides, G. & P.G. Koutsoukos. 1995. Dissolution of calcite carbonate in the presence of magnesium and orthophosphate. In Zahid Amjad (ed.), *Mineral Scale Formation and Inhibition: 73–86*. New York: Plenum Press.

Sjöberg, E.L. 1978. Kinetics and mechanism of calcite dissolution in aqueous solutions at low temperatures. *Acta Univ. Stockh. Contrib. Geol.* 332: 1–92.

Stipp, S.L.S., Eggleston, C.M. & Nielsen, B.S. 1994. Calcite surface structure observed at microtopographic and molecular scales with atomic force microscopy (AFM). *Geochim. Cosmochim. Acta* 58: 3023–3033.

Terjesen, S. G., Erga, O., Thorsen, G. & Ve, A. 1961. II. Phase boundary processes as rate determining steps in reactions between solids and liquids: The inhibitory action of metal ions on the formation of calcium bicarbonate by the reaction of calcite with aqueous carbon dioxide. *Chem. Eng. Sci.* 74: 277–288.

Van Cappellen, P., Charlet, L., Stumm, W. & Wersin, P. 1993. A surface complexation model of the carbonate mineral-aqueous solution interface. *Geochim. Cosmochim. Acta* 57: 3505–3518.